MOX–Report No. 09/2012

Adaptive geometrical multiscale modeling for hydrodynamic problems

Mauri, L.; Perotto, S.; Veneziani, A.

MOX, Dipartimento di Matematica "F. Brioschi"
Politecnico di Milano, Via Bonardi 9 - 20133 Milano (Italy)

mox@mate.polimi.it http://mox.polimi.it

Adaptive geometrical multiscale modeling for hydrodynamic problems

Lorenzo Mauri[†], Simona Perotto[♯] and Alessandro Veneziani[♭]

January 23, 2012

[†] Arianet s.r.l., Via Gilino 9, I-20128 Milano, Italy
lorenzomauri@yahoo.it

[♯] MOX– Modellistica e Calcolo Scientifico
Dipartimento di Matematica "F. Brioschi", Politecnico di Milano
Piazza Leonardo da Vinci 32, I-20133 Milano, Italy
simona.perotto@polimi.it

[♭] Department of Mathematics and Computer Science
Emory University
400 Dowman Dr., 30322, Atlanta, GA, USA
ale@mathcs.emory.edu

Keywords: geometrical multiscale models, model adaptation, hydrodynamic simulations

AMS Subject Classification: 35Q53, 65M08

Abstract

Hydrodynamic problems often feature geometrical configurations that allow a suitable dimensional model reduction. One-dimensional models may be sometimes accurate enough for describing a dynamic of interest. In other cases, localized relevant phenomena require more precise models. To improve the computational efficiency, geometrical multiscale models have been proposed, where reduced (1D) and complete (2D-3D) models are coupled in a unique numerical solver. In this paper we consider an adaptive geometrical multiscale modeling: the regions of the computational domain requiring more or less accurate models are automatically and dynamically selected via a heuristic criterion. To the best of our knowledge, this is a first example of automatic geometrical multiscale model reduction.

1 Introduction

Typically, in hydrodynamic problems high activity regions, characterized by a wide range of spatial scales (due to shocks, wave fronts, etc.), alternate with

zones where the dynamics occurs mostly along the mainstream. Due to this heterogeneity of dynamics, a high-dimensional (complete) model is often strictly required in a small portion of the computational domain whereas a low-dimensional (reduced) model is usually sufficient elsewhere. In this paper the reference hydrodynamic model is represented by the classical shallow water equations (SWE), used to describe several physical problems of interest in environmental and hydraulic engineering (e.g., tidal flows, open channel flows, free surface flows caused by dam breaking).
The simultaneous presence of heterogeneous dynamics prompted us to resort to the so-called *geometrical multiscale* reduction (see [7]), where dimensionally heterogeneous models are coupled in order to reduce the computational costs of the simulation without affecting the overall accuracy. A similar approach has been advocated in other engineering fields, like gas dynamics in internal combustion engines and computational hemodynamics (see, e.g., [2], Chap. 11). As shown in [7], the selection of the areas associated with the different models is often a challenging task, especially in the presence of fast transients. This choice is usually done *a priori*, driven by physical considerations. The main limitation is that a non optimal assignment of the 2D and 1D areas may either affect the accuracy of the computation when 1D equations are solved in regions where a complete model would be necessary; or affect the efficiency of the computation when the solution of the complete model is actually redundant.

Aim of this paper is to provide a criterion for an automatic selection of the 2D and 1D areas. We define a heuristic modeling error indicator based on the flow fluctuations across the control volume boundaries. Then, driven by this indicator, we set a model adaptive procedure. Preliminary results suggest that the automatic procedure improves the efficiency of the geometrical multiscale model reduction in comparison with the *a priori* splitting.

2 The shallow water equations

SWE are obtained by integrating the Reynolds-averaged Navier-Stokes equations over the depth of the fluid and by assuming hydrostatic pressure distribution ([10]). They express the conservation of mass and momentum for an incompressible fluid with a free surface. Getting rid of viscosity, turbulence effects and the Coriolis force, the conservative form of SWE reads

$$\frac{\partial \mathbf{u}}{\partial t} + \nabla \cdot \mathbf{F} = \mathbf{s} \qquad \text{in } \Omega, \tag{1}$$

where $\mathbf{u} = \mathbf{u}(x, y, t)$ is the vector of the conserved variables, $\mathbf{F} = \mathbf{F}(\mathbf{u})$ is the convective flux and $\mathbf{s}$ is the source term. In 2D these quantities are defined by

$$\mathbf{u} = \begin{bmatrix} h \\ hv \\ hw \end{bmatrix}, \ \mathbf{F} = \begin{bmatrix} hv & hw \\ hv^2 + \frac{1}{2}gh^2 & hvw \\ hvw & hw^2 + \frac{1}{2}gh^2 \end{bmatrix}, \ \mathbf{s} = \begin{bmatrix} 0 \\ -gh\big(\frac{\partial b}{\partial x} + \frac{m^2 v\sqrt{v^2+w^2}}{r^{4/3}}\big) \\ -gh\big(\frac{\partial b}{\partial y} + \frac{m^2 w\sqrt{v^2+w^2}}{r^{4/3}}\big) \end{bmatrix},$$

where h is the water depth, v and w are the (horizontal) depth-averaged velocity components along the x- and y- direction, respectively, g is the acceleration due to the gravity, b measures the bottom elevation with respect to a fixed reference level, m is the Manning coefficient due to the bed roughness and r is the hydraulic radius.
In a one-dimensional setting, equation (1) still holds provided that the definitions of $\mathbf{u}$, $\mathbf{F}$ and $\mathbf{s}$ simplify in

$$\mathbf{u} = \begin{bmatrix} h \\ hv \end{bmatrix}, \quad \mathbf{F} = \begin{bmatrix} hv \\ hv^2 + \frac{1}{2}gh^2 \end{bmatrix}, \quad \mathbf{s} = \begin{bmatrix} 0 \\ -gh(\frac{db}{dx} + \frac{m^2v^2}{r^{4/3}}) \end{bmatrix},$$

respectively. Appropriate initial and boundary conditions depending on the considered hydrodynamic configuration complete equations (1).

2.1 A finite volume discretization

Godunov-type finite volume schemes are largely employed to discretize SWE on both structured and unstructured meshes (see, e.g., [9, 3, 4]). Here we use a structured quadrilateral grid $\mathcal{T}$, with a second-order Godunov-type scheme based on the Roe linearized Riemann solver and the super bee flux limiters (see, e.g., [8, 4]), combined with the 2D *corner transport upwind* (CTU) method due to Colella for multidimensional integration ([1]).

Let the cells of $\mathcal{T}$ be identified by the pairs (i, j), being $i(j)$ the cell index in the $x(y)$-direction, with the notation $\mathcal{C}_{i,j} = [x_{i-1/2}, x_{i+1/2}] \times [y_{j-1/2}, y_{j+1/2}]$. Index n refers to the time level; Δx, Δy and Δt denote the uniform size of $\mathcal{T}$ along the x- and y-direction and the time step; $\mathbf{U}^n_{i,j}$ is the numerical approximation to $\frac{1}{\Delta x\,\Delta y}\int_{\mathcal{C}_{i,j}} \mathbf{u}(x, y, t^n)\,dxdy$. The finite volume discretization in the wave propagation form reads

$$\begin{aligned} \mathbf{U}^{n+1}_{i,j} = \mathbf{U}^n_{i,j} \quad &- \quad \frac{\Delta t}{\Delta x}\Big(\mathcal{A}^+\Delta\mathbf{U}^n_{i-1/2,j} + \mathcal{A}^-\Delta\mathbf{U}^n_{i+1/2,j}\Big) \\ &- \quad \frac{\Delta t}{\Delta y}\Big(\mathcal{B}^+\Delta\mathbf{U}^n_{i,j-1/2} + \mathcal{B}^-\Delta\mathbf{U}^n_{i,j+1/2}\Big) \\ &- \quad \frac{\Delta t}{\Delta x}\Big(\mathcal{F}^n_{i+1/2,j} - \mathcal{F}^n_{i-1/2,j}\Big) - \frac{\Delta t}{\Delta y}\Big(\mathcal{G}^n_{i,j+1/2} - \mathcal{G}^n_{i,j-1/2}\Big) + \Delta t\,\mathbf{S}^n_{i,j}. \end{aligned} \tag{2}$$

Since scheme (2) is explicit, we select a time step Δt to fulfill the CFL condition. The horizontal fluctuations

$$\mathcal{A}^\pm\Delta\mathbf{U}^n_{i\mp1/2,j} = \sum_{p=1}^{3}\Big(s^p_{i\mp1/2,j}\Big)^\pm\mathcal{W}^p_{i\mp1/2,j} \tag{3}$$

measure the net effect of all the right-going waves $\mathcal{W}^p_{i-1/2,j}$ from the interface $\{x = x_{i-1/2}\} \times [y_{j-1/2}, y_{j+1/2}]$ with speed $s^p_{i-1/2,j}$ and of all the left-going waves

$\mathcal{W}^p_{i+1/2,j}$ from the interface $\{x = x_{i+1/2}\} \times [y_{j-1/2}, y_{j+1/2}]$ with speed $s^p_{i+1/2,j}$, respectively; likewise, the vertical fluctuations

$$\mathcal{B}^{\pm}\Delta\mathbf{U}^n_{i,j\mp1/2} = \sum_{p=1}^{3}\Big(s^p_{i,j\mp1/2}\Big)^{\pm}\mathcal{W}^p_{i,j\mp1/2} \tag{4}$$

take into account the net effect of all the up-going waves $\mathcal{W}^p_{i,j-1/2}$ from the interface $[x_{i-1/2}, x_{i+1/2}] \times \{y = y_{j-1/2}\}$ with speed $s^p_{i,j-1/2}$ and of all the down-going waves $\mathcal{W}^p_{i,j+1/2}$ from the interface $[x_{i-1/2}, x_{i+1/2}] \times \{y = y_{j+1/2}\}$ with speed $s^p_{i,j+1/2}$, respectively. Notice that all the fluctuations in (3) and (4) are suitably modified via the Harten-Hyman entropy fix correction to treat also transonic rarefaction waves [4].

Terms $\mathcal{F}^n_{i\pm1/2,j}$ and $\mathcal{G}^n_{i,j\pm1/2}$ in (2) include the effects related to the waves transversely propagating from the neighboring cells into $\mathcal{C}_{i,j}$: they can be distinguished into the left-going and right-going transverse waves

$$\mathcal{F}^n_{i\pm1/2,j} = -\frac{\Delta t}{2\Delta y}\mathcal{A}^{\pm}\Big[\mathcal{B}^{-}\Delta\mathbf{U}^n_{i,j+1/2} + \mathcal{B}^{+}\Delta\mathbf{U}^n_{i,j-1/2}\Big],$$

respectively, and into the down-going and up-going transverse waves

$$\mathcal{G}^n_{i,j\pm1/2} = -\frac{\Delta t}{2\Delta x}\mathcal{B}^{\pm}\Big[\mathcal{A}^{-}\Delta\mathbf{U}^n_{i+1/2,j} + \mathcal{A}^{+}\Delta\mathbf{U}^n_{i-1/2,j}\Big],$$

respectively (see Figure 1). These corrections are first-order accurate. In the sequel, we resort to a second order extension (see [4], Chap. 20).

The source term is integrated via a fractional step method (the *Godunov splitting*). We first solve the SWE with no source term on the time interval $I_n = [t^n, t^{n+1})$, with initial datum $\mathbf{U}^n = [\mathbf{U}^n_{i,j}]$; this predictor step yields an intermediate solution $\mathbf{U}^{n+1,*}$. Then, we solve the independent system of ODEs $\partial\mathbf{u}/\partial t = \mathbf{s}$ on each cell and on I_n, with initial datum $\mathbf{U}^{n+1,*}$. This corrector step provides the approximation $\mathbf{U}^{n+1}$. In particular, we use an explicit second-order Runge-Kutta scheme to solve the system of ODEs: fulfillment of the CFL condition is guaranteed by an appropriate selection of the time step.

Two types of boundary conditions are used herein: *nonreflecting* boundary conditions in correspondence with the open boundaries and *slip* conditions along the solid walls. In both the cases, we use the so-called *ghost cells*. At the beginning of each time step, the values of the solution in the ghot cells are determined by an appropriate extrapolation of the solution at the previous steps or of the boundary conditions. In particular, we add two ghost cells along $\partial\Omega$ and we employ a zero-order extrapolation to set values here (see [4] for further details).

3 The adaptive geometrical multiscale solver

In this section we consider a geometrical multiscale formulation. This means that equations (1) for both the 1D and 2D domains are numerically coupled.

Our goal is an *automatic* detection of the areas of Ω where the water dynamics needs to be described with a 2D model or can be modelled by a 1D problem. To this aim, we need a modeling error indicator; then we set a modeling adaptive procedure driven by such an indicator to get the 2D-1D SW model.

3.1 Heuristic modeling error estimate for the SWE

Two different error indicators are devised to estimate: *a)* in 2D subdomains the possible reduction to 1D (model coarsening); *b)* in 1D subdomains the possible expansion to 2D (model refinement). They are both heuristic indicators and are based on the concept of fluctuation introduced in (3)-(4). In particular, we assume as reference hydrodynamic configuration an open rectilinear channel characterized by a constant rectangular cross-section and subdivided into $N_x \times N_y$ cells, slip conditions being assigned along the solid walls.

Model coarsening. Let us focus on the i-th column of cells and, in particular, on relation (2) which updates the value of $\mathbf{U}$ on the cell $\mathcal{C}_{i,j}$ at $t = t^{n+1}$. For simplicity, we assume here that the source term $\mathbf{S}^n_{i,j}$ is zero.

As indicator driving the model coarsening we assume the value $|\mathcal{B}^{\pm}\Delta\mathbf{U}^n_{i,j\mp1/2}|$ of the vertical fluctuations: if they are small, i.e.,

$$|\mathcal{B}^{\pm}\Delta\mathbf{U}^n_{i,j\mp1/2}| \leq \mathbf{Toll}_{1D} \qquad \forall j = 1,\dots,N_y, \tag{5}$$

then the i-th column is marked to be assigned to the 1D model at $t = t^{n+1}$ (see Figure 1). Notice that $\mathbf{Toll}_{1D} \in \mathbb{R}^3$ since the coarsening check has to be tested for each component of $\Delta\mathbf{U}^n_{i,j\mp1/2}$.

Let us provide some rationale behind criterion (5), referring to [6] for further details. Let us assume that the fluctuations $\mathcal{B}^{\pm}\Delta\mathbf{U}^n_{i,j\mp1/2}$ are identically equal to zero, for $j = 1,\dots,N_y$. Then, the third term on the right-hand side in (2) as well as the terms $\mathcal{F}^n_{i\pm1/2,j}$ vanish. To decide whether also the down-going and up-going transverse waves may be ignored, we consider the $(i-1)$-th and $(i+1)$-th columns, where we assume that the vertical fluctuations are equal to zero as well. It can be empirically inferred that, if $\mathcal{B}^{\pm}\Delta\mathbf{U}^n_{k,j\mp1/2} = 0$ for $k = i-1, i, i+1$ and $j = 1,\dots,N_y$, then, in those three columns, w vanishes while the water depth h is column-wise constant. Physically, this is consistent with two cases: *i)* h and v are constant along the x-direction: the horizontal fluctuations $\mathcal{A}^{\pm}\Delta\mathbf{U}^n_{i\mp1/2,j}$ and the transverse waves $\mathcal{G}^n_{i,j\pm1/2}$ vanish, so that equation (2) reduces to $\mathbf{U}^{n+1}_{i,j} = \mathbf{U}^n_{i,j}$ and no vertical fluctuation is expected in the i-th column at time $t = t^{n+1}$; *ii)* h and v are constant along the y-direction: $\mathcal{A}^{+}\Delta\mathbf{U}^n_{i-1/2,j} = \mathcal{A}^{-}\Delta\mathbf{U}^n_{i+1/2,j}$ and $\mathcal{G}^n_{i,j+1/2} = \mathcal{G}^n_{i,j-1/2}$, so that (2) reduces to

$$\mathbf{U}^{n+1}_{i,j} = \mathbf{U}^n_{i,j} - \frac{\Delta t}{\Delta x}\Big(\mathcal{A}^{+}\Delta\mathbf{U}^n_{i-1/2,j} + \mathcal{A}^{-}\Delta\mathbf{U}^n_{i+1/2,j}\Big) \tag{6}$$

and no vertical fluctuation is expected in the i-th column at time $t = t^{n+1}$. Should h and v vary along both x- and y-direction, the four terms $\mathcal{A}^{\pm}\Delta\mathbf{U}^n_{i\mp1/2,j}$,

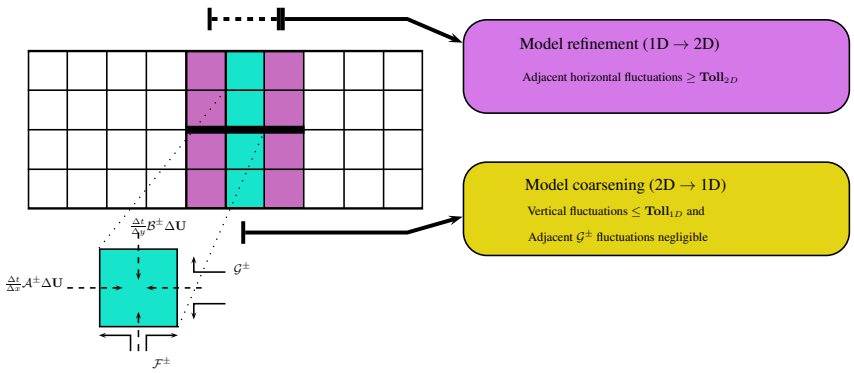

Figure 1: Fluctuations driving the modeling adaptive procedure

$\mathcal{G}^n_{i,j\pm1/2}$ do not vanish and vary for different values of j. So we infer that this assumption is not compatible with the condition that the vertical fluctuations in the current and adjacent columns vanish.

In practice, condition $\mathcal{B}^{\pm}\Delta\mathbf{U}^n_{i,j\mp1/2} = 0$ is relaxed and turns into criterion (5). If this check holds for the $(i-1)$-th, i-th and $(i+1)$-th column, then the i-th column is eligible to be associated with the 1D model. At this point equation (6) is solved by assuming for $\mathbf{U}^n_{k,j}$, with $k = i, i \pm 1/2$, the mean value of $\mathbf{U}^n_{k,j}$ over the k-th column.

Model refinement. It is less immediate to find a reliable criterion driving the refinement of the 1D areas. In principle one should quantify the vertical fluctuations but, of course, these quantities are not computed by a one-dimensional model.

Thus, we focus on the horizontal fluctuations with the following idea: high horizontal fluctuations in the neighborhood of an element are likely to transfer energy along the vertical direction, triggering a significant vertical component of the velocity. At $t = t^n$, we compute therefore the entity of horizontal fluctuations in all the columns associated with the 2D model and neighboring with a 1D segment: if they are large enough, the 1D domain becomes eligible to be associated with the 2D model. In more detail, if the i-th column is adjacent, on the right, to a 1D segment and $|\mathcal{A}^{+}\Delta\mathbf{U}^n_{i+1/2,j}|$ is sufficiently large, for some $j = 1, \ldots, N_y$, then the 1D segment becomes a candidate to be a (the $(i+1)$-th) 2D column; likewise if the i-th column is adjacent, on the left, to a 1D segment and $|\mathcal{A}^{-}\Delta\mathbf{U}^n_{i-1/2,j}|$ is sufficiently large, for some $j = 1, \ldots, N_y$, then the 1D segment becomes eligible to be a (the $(i-1)$-th) 2D column (see Figure 1).

The error indicator driving the model refinement is consequently represented by the horizontal fluctuations $\mathcal{A}^{\pm}\Delta\mathbf{U}^n_{i\pm1/2,j}$; the corresponding refinement criterion reads: if

$$|\mathcal{A}^{\pm}\Delta\mathbf{U}^n_{i\pm1/2,j}| \geq \mathbf{Toll}_{2D} \qquad \text{for some } j = 1, \ldots, N_y, \tag{7}$$

then the 1D segment at the right (at the left) of the i-th column is marked to be

assigned to the 2D model at $t = t^{n+1}$. As in (5), $\mathbf{Toll}_{2D} \in \mathbb{R}^3$ and the refinement check has to be verified for each component of $\Delta\mathbf{U}^n_{i\pm1/2,j}$.

3.2 The modeling adaptive procedure

This procedure moves from the coarsening and the refinement criteria above to set up an automatic selection of the 2D and 1D areas. We can itemize the generic k-step of the modeling adaptive procedure we propose in such a way: running over all the N_x columns,

1. we mark all the 2D columns where criterion (5) holds as eligible for the 1D model and we group the consecutive columns thus marked;

2. we mark all the 1D intervals neighboring with a 2D column where one of the criteria (7) holds as eligible for the 2D model and we group the consecutive intervals thus marked;

3. we select the groups in 1. and 2. which are neighbors with sets of at least $min2d$ 2D columns and/or sets of at least $min1d$ subintervals;

4. all the groups identified by 1. and 3. constituted by at least q columns, with $q \geq min1d$, are assigned to the 1D model;

5. all the groups identified by 2. and 3. constituted by at least p subintervals, with $p \geq min2d$, are assigned to the 2D model.

This approach guarantees always a minimum size for both the 2D and 1D areas given by $min2d \cdot \Delta y$ and $min1d \cdot \Delta x$, respectively. Moreover, we permanently associate a certain area of the domain with the 2D model in the presence of a hydrodynamic configuration (e.g., a pillar, a pier) or a boundary condition (e.g., a lateral inlet) which implicitly induces vertical fluctuations.

Concernig the matching conditions between the two classes of models, we distinguish *1D-2D* and *2D-1D couplings*. For the former, we extend the 1D values of h and hv to all the N_y cells in the first column of the 2D domain, while setting $hw = 0$. For the latter, the mean value of h and hv over the N_y cells in the last column of the 2D domain is assigned to the corresponding 1D variables. Alternative and more sophisticated approaches are discussed in [6], also suitable in the presence of a source term. Notice that empirical criteria (5) and (7) rely on the assumption of no-forcing term. Should a forcing term be on, these criteria need to be properly modified [6].

The same time step Δt for both the 2D and the 1D domains is selected so that the CFL condition is globally fulfilled. Finally, to contain the computational cost of the whole adaptive procedure, we update the 2D/1D model every M^* time-steps instead at each time step.

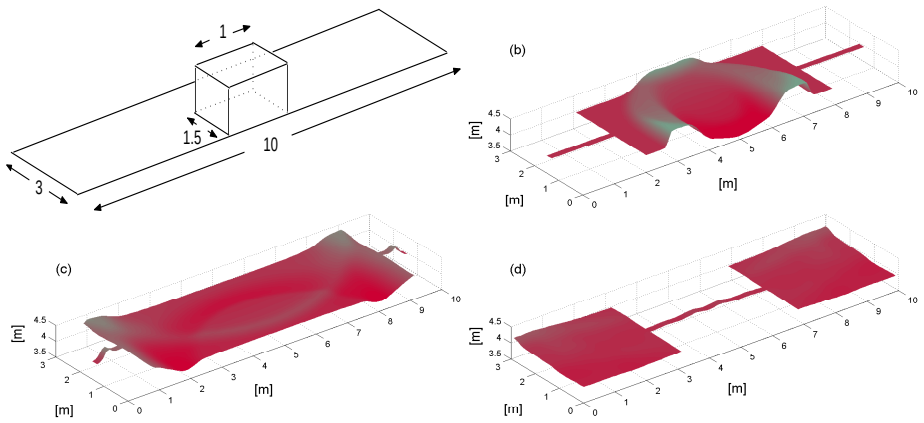

Figure 2: Adaptive geometrical multiscale modeling: test case sketch (top-left); 3D representation of the free surface at $t = 1$s (top-right), $t = 2$s (bottom-left), $t = 10$s (bottom-right)

Numerical validation. With this test case we analyze the proposed modeling adaptive procedure, essentially from a qualitative viewpoint. We have implemented the adaptive solver in Clawpack 4.3 ([5]). We consider a popular hydrodynamic benchmark, i.e., a rectangular dam-break simmetrically localized in a 10m $\times$3m rectangular channel with a flat horizontal frictionless bed (see Figure 2, top-left). The dam break occurs due to the istantaneous collapse of three of the dam walls. We employ a grid consisting of 100×30 cells, we assign slip boundary conditions on the whole $\partial\Omega$, and we set 1 as maximum value for the CFL condition. Concerning the parameters involved in the modeling adaptive procedure, we set: $\mathbf{Toll}_{1D} = \mathbf{Toll}_{2D} = [10^{-1}, 10^{-1}, 10^{-1}]^T$, $min2d = 10$, $min1d = 2$, $M^* = 5$.
In Figure 2 we show the water surface for three different times: the 2D model follows the evolution of the dynamics as well as that the intrisic symmetry of the problem is preserved by the model adaptation.

For a more quantitative investigation of the modeling adaptive procedure we refer to [6].

References

[1] Colella, P.: Multidimensional upwind methods for hyperbolic conservation laws. J. Comput. Phys. **87**, 171–200 (1990)

[2] *Cardiovascular Mathematics, Modeling and Simulation of the Circulatory System.* In: Formaggia, L., Quarteroni, A., Veneziani, A. (eds.), Modeling Simulation and Applications **1**, Springer, Milano (2009)

[3] Krámer, T., Józsa, J.: Solution-adaptivity in modelling complex shallow flows. Computers & Fluids **36**, 562–577 (2007)

[4] LeVeque, R.J.: *Finite Volume Methods for Hyperbolic Problems*. Cambridge, (2001).

[5] LeVeque, R.J.: Clawpack, Version 4.3. http://depts.washington.edu/clawpack/clawpack-4.3/

[6] Mauri, L., Perotto, S., Veneziani, A.: An adaptive geometrical multiscale model for the shallow water equations. In preparation (2012)

[7] Miglio, E., Perotto, S., Saleri, F.: Model coupling techniques for free-surface flow problems. Part I. Nonlinear Analysis, **63**, 1885–1896 (2005)

[8] Roe, P.L.: Approximate Riemann solvers, parameter vectors, and difference schemes. J. Comput. Phys. **43**, 357–372 (1981)

[9] Sleigh, P.A., Berzins, M., Gaskell, P.H., Wright, N.G.: An unstructured finite volume algorithm for predicting flow in rivers and estuaries. Computers & Fluids **27**, 479–508 (1998)

[10] Vreugdenhil, C.B.:*Numerical Methods for Shallow-Water Flow*. Springer, (1994).

MOX Technical Reports, last issues

Dipartimento di Matematica "F. Brioschi",
Politecnico di Milano, Via Bonardi 9 - 20133 Milano (Italy)

09/2012 Mauri, L.; Perotto, S.; Veneziani, A.
Adaptive geometrical multiscale modeling for hydrodynamic problems

08/2012 Sangalli, L.M.; Ramsay, J.O.; Ramsay, T.O.
Spatial Spline Regression Models

07/2012 Perotto, S; Zilio, A.
Hierarchical model reduction: three different approaches

06/2012 Micheletti, S.; Perotto, S.
Anisotropic recovery-based a posteriori error estimators for advection-diffusion-reaction problems

05/2012 Ambrosi, D; Arioli, G; Koch, H.
A homoclinic solution for excitation waves on a contractile substratum

04/2012 Tumolo, G.; Bonaventura, L.; Restelli, M.
A semi-implicit, semi-Lagrangian, p-adaptive Discontinuous Galerkin method for the shallow water equations

03/2012 Fumagalli, A.; Scotti, A.
A reduced model for flow and transport in fractured porous media with non-matching grids

02/2012 Arioli, G.
Optimization of the forcing term for the solution of two point boundary value problems

01/2012 Lassila, T.; Manzoni, A.; Quarteroni, A.; Rozza, G.
A reduced computational and geometrical framework for inverse problems in haemodynamics

47/2011 Antonietti, P.F.; Borz, A.; Verani, M.
Multigrid shape optimization governed by elliptic PDEs